Diurnal, weekly, seasonal and spatial variabilities in carbon dioxide flux in different urban landscapes in Sakai, Japan

Masahito Ueyama[1], Tomoya Ando[1]

[1] Graduate School of Life and Environmental Sciences, Osaka Prefecture University, Sakai, 599-8531, Japan

5   *Correspondence to*: Masahito Ueyama (miyabi-flux@muh.biglobe.ne.jp)

Abstract. To evaluate CO_2 emissions in urban areas and their temporal and spatial variabilities, continuous measurements of CO_2 fluxes were conducted using the eddy covariance method at three locations in Sakai, Osaka, Japan. Based on the flux footprint at the measurement sites, CO_2 fluxes from the three sites were partitioned into five datasets representing a dense urban center, a moderately urban area, a suburb, an urban park, and a rural area. Distinct biological uptake of CO_2 was

10   observed in the suburb, urban park, and rural areas in the daytime, whereas high emissions were observed at dense and moderate urban areas in daytime. Weekday CO_2 emissions in the dense urban center and suburban area were approximately 50% greater than during weekend and holidays, but the other landscapes did not exhibit a clear weekly cycle. Seasonal variations in the urban park, rural area, and suburban area were influenced by vegetation activities, exhibiting the lowest daily emissions or even uptakes during summer months. In contrast, the dense and moderately urban areas exhibited higher

15   emissions in winter and summer months, when emissions significantly increased as air temperature increased in summer and air temperature decreased in winter. Irrespective of the landcover type, all urban landscapes measured in this study acted as net annual CO_2 sources, with emissions ranging from 0.5 to 4.9 kg C m^{-2} yr^{-1}. The magnitude of the annual CO_2 emissions was negatively correlated with green fraction; areas with a smaller green fraction had higher annual CO_2 emissions. Upscaled flux estimates based on the green fraction indicated that the emissions for the entire city were 3.3 kg C m^{-2} yr^{-1},

20   which is equivalent to 0.5 Tg C yr^{-1} or 1.8 Mt CO_2 yr^{-1} based on the area of the city (149.81 km^2). A network of eddy covariance measurements is a powerful tool to evaluate CO_2 emissions from urban areas.

1 Introduction

Cities emit a considerable amount of carbon dioxide (CO_2) that is associated with human activities into the atmosphere (Canadell et al., 2007). Urban areas account for only a samll percentile of the earth's land surface but emit 30–50% of total

25   anthropogenic CO_2 (Mills, 2007; Stterthwaite, 2008). Consequently, CO_2 emissions from cities are highly heterogeneous at spatial and temporal scales.

Global CO_2 emissions have often been estimated using inventories (Oda and Maksyutov, 2011). The major challenge for estimating global CO_2 emissions is to understand the spatio-temporal dynamics of CO_2 emissions in various cities. Because

emissions data are used in top-down estimates of global CO_2 budget (Peters et al., 2007; Schmel et al., 2001), a better estimate of CO_2 emissions from cities will improve our understanding of global carbon cycle, including terrestrial and ocean fluxes.

5   To evaluate CO_2 emissions in cities and their temporal and spatial variabilities, continuous measurements of CO_2 fluxes have been conducted using the eddy covariance method in various urban landscapes, including dense urban built-up area (Gioli et al., 2012; Grimmond et al., 2002, 2004; Kotthaus and Grimmond, 2012; Nimitz et al., 2002; Pawlak et al., 2011; Velasco et al., 2005), suburban areas (Bergeron and Strachan, 2011; Coutts et al., 2007; Crawford et al., 2011; Hirano et al., 2015; Moriwaki et al., 2006; Ward et al., 2013), urban parks (Kordowski and Kuttler, 2010), and urban forests (Awal et al., 2010),

10   in several cities. These results indicated that cities emits a considerable amount of CO_2 into the atmosphere associated with human activities, such as vehicle traffic and household heating in the wintertime.

Multi-site eddy covariance towers were used to synthesize the data and showed that vegetation fraction was the major factor controlling spatial variability in annual CO_2 emissions (Nordbo et al., 2012; Velasco and Roth, 2010; Ward et al., 2015)

15   because vegetation fraction can be correlated with anthropogenic activities. Upscaling can provide a high-resolution map of direct CO_2 emissions from cities. Previous studies have examined the relationship between annual CO_2 emissions and vegetation fraction at a global scale (Nordbo et al., 2012; Velasco and Roth, 2010; Ward et al., 2015). It is unclear whether upscaling CO_2 emissions is possible within a city, because multi-site eddy covariance measurements within a city are often unavailable.

In this study, we present diurnal, weekly, seasonal, and spatial variabilities in CO_2 flux continuously measured at three different locations within 5 km of each other in Sakai, Osaka, Japan. Considering flux footprint, the data represent five urban landscapes, including a dense urban center, a moderately urban area, a suburb, a rural area, and an urban park. Regardless of the landscape type, all landscapes emitted considerable CO_2 annually with different temporal metabolisms, providing a

25   useful overview of anthropogenic CO_2 emissions.

2 Materials and methods

2.1 Study sites

Sakai is the second largest city in Osaka Prefecture, located in western Japan. The population was approximately 842,000 in 2015. Because the city is located on the eastern shore of Osaka Bay, sea breeze circulation is evident throughout the year

30   except when seasonal winds are not strong. The area is on a uniformly flat plane; the north-south and the east-west slopes are 0.0030° and 0.0024°, respectively. The climate of Sakai is temperate; the mean annual air temperature is 15.9°C, the maximum monthly mean air temperature is 28.0°C in August, the minimum monthly mean air temperature is 5.2°C in

January, and the mean annual precipitation is 1187 mm yr^{-1} between 1981 and 2010 according to the apanese Meteorological Agency.

The Sakai city center (SAC) site (Fig. 1; Table 1) is located on a tower at the top of a city office building (34°34′25″N, 135°28′80″E). The population density around the city center is approximately 12150 km^{-2}, based on the Japanese Government Statistics. The area is a densely built-up urban area with a mean building height of 10.7 ± 3.1 m. Many arterial roads and two highways with heavy traffic are present within the flux footprint. Because industrial and commercial areas are located in the western and northern parts of the city, those areas are expected to show higher rates of human activity than locations where residential areas are dominant.

The Oizumi Ryokuchi urban park (IZM) site (Fig. 1; Table 1) is located at the northern end of the city (34°33′48″N, 135°32′1″E), and was established in 1972. The measurements were conducted at a tower located at the east edge of the park. Because of the consistent presence of a sea breeze, the tower is mostly located downwind direction of the park during the daytime. The landcover of the park consists of 51% trees, 15% grassland, and 34% other. Measurements using a plant canopy analyzer (LAI-2000, LI-COR, Lincoln, Nebraska, USA) showed that the leaf area index of trees ranged from 3.2 to 5.7 m^2 m^{-2} with a mean of 4.3 m^2 m^{-2} in the summer months. The area surrounding the IZM is a mixed landscape of residential area and agricultural fields and is characterized as a rural area.

The Osaka Prefecture University (OPU) site (Fig. 1; Table 1) is located at the west edge of Osaka Prefecture University (34°32′50″N, 135°30′10″E). Because the measurements were conducted at the roof top of a building, the flux footprint represents only a small suburban area. The western part of the site contains a protected forest on an ancient tumulus, Mozu Kofungun. The area is characterized as a suburb, consisting of a university, a residential area, small streets, a graveyard, and trees.

2.2 Observations

We measured CO$_2$ fluxes using the eddy covariance method at the three sites. For SAC, a sonic anemometer (SAT550, Sonic Corp., Tokyo, Japan) and an open-path infrared gas analyzer (LI-7500, LI-COR) were installed on a 16-m tower located at the top of the city office building (111 m above the ground) at the end of November, 2009 (Ueyama et al., 2011). For IZM, a sonic anemometer (CSAT3, Campbell Scientific Inc., Logan, Utah, USA) and an open-path infrared gas analyzer (EC150, Campbell Scientific Inc.) were installed 30 m above the ground on a tower at the end of January 2015. For OPU, sonic anemometers and several infrared gas analyzers were installed on a 2-m mast above the rooftop at the edge of the building (16.2 m above the ground) in November 2014. Turbulent fluctuations were recorded at 10Hz using a datalogger (CR1000, Campbell Scientific Inc.).

For the OPU site, eddy covariance systems were periodically changed. A sonic anemometer (DA600, Sonic Corp.) was in place from November 2014 to March 2015 and again in November 2015. A different sonic anemometer (Model 81000, R. M. Young, Traverse, Michigan, USA) was in place from March 2015 to April 2015, and a third type of sonic anemometer

5   (Windmaster, Gill Instruments, Lymington, UK) was in place in April 2015. The eddy covariance system was initially a closed-path system using a gas analyzer (LI-6262, LI-COR), until March 2015, and was then changed to an open path system using an open-path infrared gas analyzer (LI-7500, LI-COR). Another eddy covariance system using a sonic anemometer (DA600, Sonic Corp.) and an open-path infrared gas analyzer (LI-7500, LI-COR) was installed on a different edge of the building in November 2015. This additional measurement system increased data acquisition, because we eliminated the data

10 coming from the roof. Consequently, CO_2 fluxes were calculated based on the different systems with relevant corrections. We confirmed that there was no significant difference between open-path and closed-path systems through an inter-comparison, but these flux measurements have higher uncertainties than those from the other sites.

Meteorological and environmental variables were measured at each site. Air temperature, relative humidity, and incoming

15 solar radiation were measured at the three sites. Rainfall, atmospheric pressure, incoming longwave radiation, and ground heat fluxes at the top of the building were measured at OPU. Leaf area index was manually measured approximately once a month using a plant canopy analyzer (LAI-2000, LI-COR) at ten forested sectors in IZM.

2.3 Data analysis

Turbulent fluxes were calculated using the eddy covariance method using the Flux Calculator program (Ueyama et al., 2012).

20 Before the half-hourly covariance of vertical wind velocity and scalar quantities was calculated, spike data were removed from the raw data. No trend removal was applied. The artificial fluctuations of sonic air temperature associated with water vapor were corrected. Vertical wind velocity was coordinated as mean vertical wind velocity was zero using the double rotation method. The angle-of-attack errors for the Gill Instruments and R. M. Young anemometers were corrected based on Nakai and Shimoyama (2012) and Kochendorfer et al. (2012), respectively. The high-frequency loss for line averaging and

25 sensor separation was corrected using theoretical transfer functions for the open-path systems (Massman, 2000) and empirical transfer functions for the closed-path system (Moore, 1986). Air density fluctuations were corrected based on Webb et al (1980).

Filtering nighttime data using friction velocity (u_*) threshold was not applied in this study. This was because (1) no clear

30 threshold was obtained in nighttime data, (2) data coverage at night was small due to the limited flux footprint, and (3) sensible heat fluxes in summer months often showed positive values even at night except IZM. Our handling of nighttime data was the same in previous studies in urban areas (e.g., Liu et al., 2012), but a potential underestimate of nighttime fluxes may have occurred.

Flux data were selected for each landscape after a quality test and footprint analysis. First, we applied the quality test to remove half-hourly flux data that included noise based on a criterion (Appendix B.1 in Ueyama et al., 2012). A stationary test, integral turbulence test, and higher moment test were applied. The fluxes, measured when winds came from the tower directions, were also removed. For OPU, the fluxes, measured when winds came from the directions of the building, were removed as well. For SAC, based on a footprint model (Kormann and Meixner, 2000), we rejected a data, when the source area contributing 80% of the flux footprint contained sea and mountains. Similarly, for IZM, we rejected flux data, when the source area contributing 50% of the flux footprint exceeded the boundary of the urban park.

Depending on wind directions, flux data at IZM and SAC were divided into two data series. For IZA, flux data from the west represented the urban park, whereas data from other directions represented the rural area consisting of mixed residential and agricultural areas (Fig. 1). For SAC, flux data from the west represented the densely built-up urban center, whereas data from other directions represented the moderate urban to residential area (Fig. 1). Consequently, we formed five flux datasets from measurements at the three sites: a dense urban center (west SAC), a moderately urban area (east SAC), a suburb (OPU), an urban park (west IZM), and a rural area (east IZM). Data coverage was 11% in west SAC, 21% in east SAC, 31% in OPU, 16% in west IZM, and 13% in west IZM.

Partitioning CO_2 fluxes into assimilatory and respiratory fluxes was conducted only for the west and east IZM and OPU datasets, because biological signals were present in CO_2 fluxes. The flux partitioning was conducted using the Flux Analysis Tool program (Ueyama et al., 2012). First, the relationship between nighttime CO_2 fluxes and air temperature was established based on a model (Lloyd and Taylor, 1994). The relationship was determined daily with a 49-day moving window. Assimilatory fluxes were calculated as the difference between the estimated respiratory flux and the measured CO_2 flux. Because the estimated respiratory fluxes consisted of biological fluxes and nighttime anthropogenic fluxes, it is important to note that the estimated assimilatory fluxes did not truly represent gross primary productivity, which is often used in ecosystem studies (e.g., Baldocchi, 2008).

Gaps in the five datasets were filled using the Flux Analysis Tool program. First, small data gaps for periods less than 2.0 h were filled by linear interpolation. Second, for the west and east IZM datasets, gaps were filled using a combination of look-up-table and non-linear regression methods (Ueyama et al., 2012), an approach well established for use in natural ecosystems (Ueyama et al., 2013).For data gaps from west and east SAC and OPU, mean diurnal variations were applied, in which a mean diurnal pattern was created daily using a 51-day moving window. Two mean diurnal patterns were created, one for weekdays and once for weekends and holidays according to the weekly cycle.

The potential mitigation of CO_2 uptake by vegetation (R_M) was inferred for west and east IZM and OPU using the followings:

$$R_M = \varepsilon\, F_A / \left(F_{NUE} + \varepsilon\, F_A \right) \qquad (1)$$

where F_A represents the partitioned assimilatory flux, F_{NUE} represents CO_2 emissions measured by the eddy covariance, and ε represents the conversion efficiency of gross assimilation into net assimilation (0.06; Baldocchi, 2008). The value of ε was determined based on a global synthesis of disturbed ecosystems, although there is considerable uncertainty in its use with urban vegetation. Furthermore, the estimated F_A may be biased due to nighttime anthropogenic activities.

10 **2.4 Upscaling using GIS data**

The annual CO_2 flux was upscaled according to the relationship between annual fluxes and green fraction. The green fraction was estimated using a green census data developed by government of Sakai City. The green census data were created using high-resolution aerial photographs from August 2001 consisting of polygons of approximately 5-m spatial resolution. Based on the high-resolution polygon data, the green fraction was evaluated at a 500-m spatial resolution. Because the green census 15 data often classified water area as green area, we masked water area using landcover data based on a geographical information system (Digital Map 5000 for the Kinki region in 2008 by the Geospatial Information Authority of Japan).

3 Results

3.1 Diurnal variations

CO_2 fluxes showed distinct diurnal variation (Fig. 2). At the IZM, in the urban park and rural area, distinct biological signals 20 were observed, representing apparent daytime uptake. The magnitude of the daytime uptake was stronger in the urban park than in the rural area. A daytime uptake was also observed at OPU in the summer months from April to August. In contrast to the apparent biological signals, diurnal variations at SAC showed greater CO_2 emissions during the daytime than at night. Emissions were greater in the dense urban center (west SAC) than in the moderately urban area (east SAC). Emissions from the urban areas tended to be high in the daytime, particularly in the morning rush hours. Such diurnal variations were similar 25 to those for traffic counts measured by highway exits within the flux footprint (Fig. 2b). Note that the traffic counts at the exits peaked in the evening, whereas those at the entries could peaked in the morning (data are not shown).

3.2 Seasonal variations

Different urban landscapes showed different seasonal variations in CO_2 flux (Fig. 3). Similar to the diurnal variations, distinct biological signals were observed at IZM in the urban park and rural area. The daily mean CO_2 flux showed lower 30 emissions with occasional negative values during summer months in both IZM sites. The suburban site of OPU generally

showed CO_2 emissions throughout the seasons, but the emissions rate tended to be lower in the spring than in other months. The SAC site showed high CO_2 emissions throughout the seasons, and higher emissions were observed in the dense urban center than in the moderately urban area. The seasonal variations in SAC exhibited two distinct peaks during the summer and winter periods.

The seasonal variations in the daily CO_2 flux were dependent on daily mean air temperature and exhibited different patterns in different landscapes (Fig. 4). For the urban site of SAC, CO_2 emissions increased as temperatures decreased (0.46-0.27 g C m^{-2} d^{-1} $°C^{-1}$; $p < 0.1$) when mean daily temperature less than 10°C. Higher CO_2 emissions were also observed at higher temperatures at SAC. An increase in CO_2 emissions at higher temperatures was also observed at OPU. Gas consumption by university buildings within a footprint of OPU was consistent with the two seasonal peaks revealing higher consumption in the summer and winter months (Fig. A1). In the urban park and rural area, CO_2 emissions decreased as temperatures increased above 20°C.

Assimilatory fluxes were greater in summer months than in winter months (Fig. 3). Surprisingly, the assimilatory fluxes in the urban park and OPU were comparable, probably due to contributions of trees around the university and from the tomb at OPU. The assimilatory fluxes for the rural area were approximately half those for the urban park and OPU. The assimilatory fluxes increased as temperatures increased higher than 20°C at 0.15-0.38 g C m^{-2} d^{-1} $°C^{-1}$ ($p < 0.01$).

3.3 Weekly variations

Among the five landscapes, distinct weekly cycles of CO_2 emissions were only observed at the west SAC and OPU sites (Fig. 5). On average, CO_2 emissions on weekdays were approximately 50% greater than emissions on weekends and holidays, even though the weekday CO_2 flux at the east SAC tended to be 10% higher than the fluxes on holidays. The greater emissions on weekdays were consistently observed throughout all seasons, and were consistent with the traffic counts from the highway exits, where traffic was approximately 23% higher on weekdays than on weekends and holidays (Fig. 2b).

3.4 Annual CO_2 balance and its spatial variations

All urban landscapes measured in this study acted as net CO_2 emissions sources on the annual timescale (Fig. 6; Table 2). The strength of the annual CO_2 emissions was negatively correlated with the green fraction ($R^2 = 0.96$; $p < 0.01$); areas of a smaller green fraction had higher annual CO_2 emissions. Based on the annual assimilatory fluxes and annual CO_2 emissions measured using Equation 1, the potential mitigation of CO_2 uptake by urban vegetation ranged from 5% to 9% (Table 2). This pattern indicates that direct mitigation by vegetation is limited and that the green fraction explains the magnitude of anthropogenic activities rather than the direct contributions from vegetative uptake. The annual CO_2 emissions estimated in this study were lower than those examined using a global synthesis by Nordbo et al. (2012) (Fig. 6).

Based on the significant relationship between the green fraction and the annual CO_2 flux, annual CO_2 fluxes were upscaled to the city scale (Fig. 7). Because the green fraction of Sakai was low in the north and high in the south (Fig. 7a), annual CO_2 emissions were greater in the north than the south (Fig. 7b). The annual CO_2 fluxes from the entire city were 3.3 kg C m^{-2} yr^{-1}, which corresponds 0.5 Tg C yr^{-1} or 1.8 Mt CO_2 yr^{-1} based on the area of the city (149.81 km^2). The estimated emissions were lower than an inventory-based estimate from 2000 to 2012 (8.0 ± 0.6 Mt CO_2 yr^{-1}) published by the government.

4 Discussion

Annual CO_2 emissions from Sakai City ranged in those measured in other studies, but tended to be at the lower end of the range (Fig. 6). For the same fraction of green area (in this case, the green fraction was less than 20%), urban emissions ranged from 4 to 18 kg CO_2 m^{-2} yr^{-1} for other cities (Nordbo et al, 2012; Velasco and Roth, 2010). The low CO_2 emissions rate in Sakai City was evident in daytime peaks during winter months (Fig. 2) compared with London (e.g., more than 50 μmol m^{-2} s^{-1}, Ward et al., 2015) and Beijing (30 μmol m^{-2} s^{-1}, Liu et al., 2012). Warmer winter temperatures may contribute to lower emissions as a result of reduced building heating and thus lower annual emissions in Sakai City compared with other northern cities. The annual emissions rate in our urban center was comparable to that of the densely populated residential area in Tokyo (4.3 kg CO_2 m^{-2} yr^{-1}, Hirano et al., 2015).

The sensitivity of the CO_2 emissions to cold temperatures was comparable to that described in the previous studies (Bergeron and Strachan, 2011; Liu et al., 2012; Pawlak et al., 2011). The effect of building heating has often been estimated as a slope between air temperature and the CO_2 emissions rate: -2.02 g C m^{-2} d^{-1} °C^{-1} in London (Ward et al., 2015), -0.21 g C m^{-2} d^{-1} °C^{-1} in Łódź (Pawlak et al., 2011), and -0.35 g C m^{-2} d^{-1} °C^{-1} in Beijing (Liu et al., 2012). These values are comparable to those obtained in our city: -0.46 to -0.27 g C m^{-2} d^{-1} °C^{-1} (Fig. 4). No sensitivities to cold temperatures were found in the urban park (west IZM), rural area (east IZM), or residential area (OPU), could be due to the mixed effects of biological and anthropogenic signals.

CO_2 emissions in urban landscapes (SAC and OPU) also increased as temperatures increased in the summer months (Fig. 4): 0.22 g C m^{-2} d^{-1} °C^{-1} in west SAC ($p = 0.01$), 0.24 g C m^{-2} d^{-1} °C^{-1} in east SAC ($p = 0.02$), and 0.13 g C m^{-2} d^{-1} °C^{-1} in OPU ($p = 0.26$). Because traffic did not show a clear seasonal variation (Fig. 2b), the reason for this increase is unclear, but one possibility is the contribution of emissions from gas-powered air conditioners (Fig. A1). The prevalence rate of gas-powered air conditioners is approximately 20% of non-residential buildings, based on an assessment by the Japan Gas Association. A weaker dependence in OPU probably occured because emissions from gas-powered air conditioners from the university building were canceled out by an increase in biological uptake (Fig. 3b). The sensitivity of assimilatory fluxes to warming temperatures was 0.38 g C m^{-2} d^{-1} °C^{-1} in OPU ($p < 0.01$).

Weekly cycles of CO_2 emissions were only observed at urban sites (Fig. 5), representing the strength of human activities. Previous urban CO_2 flux studies reported that major contributors to anthropogenic emissions were vehicle emissions and gas consumption (Gioli et al., 2012; Hirano et al., 2015; Velasco et al., 2005; Ward et al., 2013). Velasco and Roth (2010) indicated that weekly cycles were primarily related to vehicle emissions. Traffic count was high on weekdays at SAC (Fig. 2b), and business offices including the university are often more active on weekdays than weekends and holidays. In contrast, there were no clear weekly cycle in east SAC, urban parks, and rural areas. Lager differences between weekday and holiday in west SAC and OPU suggest the greater contributions of emissions from vehicles and business offices compared with other landscapes. This underscore the importance of temporal variations in CO_2 emissions by land use.

The role of the urban park in migrating urban CO_2 emissions was limited. Several factors explain the annual emissions from the urban park. First, the urban park frequently suffered from various management activities, such as harvesting and weeding. Such frequent disturbances could decrease sink and increase source (Gough et al., 2007; Latty et al., 2004). Warmer climates in the urban area may induce higher respiration (Awal et al., 2010). A limited footprint might influence CO_2 fluxes arising from emissions from surrounding areas. We re-checked the data selection using stricter criteria according to which we rejected data when 80% of the flux footprint exceeded boundary of the urban park, but the results were almost the same. A positive CO_2 budget of 2400 g CO_2 m^{-2} yr^{-1} was previously measured at an urban park in Germany (Kordowski and Kuttler, 2010).

Partitioning flux data measured at a single site with distinct landscapes is a useful approach in urban flux studies. CO_2 fluxes at different landscapes measured at a single site showed considerably different behaviors (Fig. 2, 3, 6). The approach previously used for clarifying variations in fluxes in different landscapes involved single flux measurements (Järvi et al., 2012; Kordowski and Kuttler, 2010; Hirose et al., 2015). The partitioning concurrently contained limitations that data availability decreases with partitioning. In the study area, sea-breeze circulation was dominant in the summer months, resulting in a large data gap from certain wind directions (shown in section 2-3). Accumulating long-term data could be useful for filling the data gap.

The green fraction can be useful for upscaling annual CO_2 flux in urban area (Fig. 6). Our study indicated that direct mitigation by vegetation was limited in terms of partitioned assimilatory flux (Fig. 3b); thus, the green fraction was an index of human activities. The applicability of the green fraction was previously reported based on a global synthesis based on the eddy covariance measurements in urban areas (Nordbo et al., 2012; Velasco and Roth, 2010; Ward et al., 2015). The relationship between the annual CO_2 flux and the green fraction in Sakai City tended to be lower than the relationship revealed by the global synthesis (Nordbo et al., 2012) (Fig. 6). This difference might indicate that the relationship differs in each city or country. Consequently, to quantify the effects of the green fraction on CO_2 emissions in various cities, further direct measurements of CO_2 flux at various urban sites are required.

Upscaled annual CO_2 fluxes for the city (Fig. 7) were lower than estimated using the inventory published by the government. According to the inventory, approximately 57% of CO_2 emissions were associated with the industrial sector, but there was no eddy covariance site in the coastal industrial region. Part of the discrepancy occurred because our upscaling estimated the net flux of urban emissions and vegetative uptake, whereas the inventory quantified the emissions. Hirano et al. (1996) estimated that vegetation in Sakai, primarily in southern sectors, absorbed 0.87 Mt CO_2 yr^{-1} of CO_2 based on an inventory-based estimates. Another reason for the discrepancy was that our estimate did not include hot spot emissions, such as power plants and incineration facilities, or non- CO_2 gas emissions. Oda and Maksyutov (2011) estimated that approximately half of annual total CO_2 emissions were from point sources in most countries. Because our upscaled CO_2 flux did not include such point sources, CO_2 emissions from point sources could be more rigorously quantified using the governmental inventory than non-point sources (Oda and Maksyutov, 2011). Thus, upscaled CO_2 flux could be useful as an additional constraint, providing more information regarding CO_2 emissions from non-point sources. This method could be useful for estimating regional CO_2 emissions when combined with inventory estimates.

5 Conclusion

Based on continuous measurements using the eddy covariance method at three different urban sites, diurnal, weekly, seasonal, and spatial variabilities in CO_2 flux were evaluated in Sakai, Osaka, Japan. The urban center and university sites acted as CO_2 sources throughout seasons. A clear weekday/holiday cycle of CO_2 emissions was observed at those sites. A diurnal pattern in the urban center was correlated with those for traffic count. High emissions were observed in the urban site in both winter and summer months, even though the traffic did not change seasonally, suggesting that changes in gas consumption influenced the seasonal variabilities. The urban park and rural area exhibited CO_2 uptake during summer months, with distinct daytime uptake. Regardless of the green fraction, all landscapes considered in this study acted as an annual CO_2 source. Previous studies of the relationship between annual CO_2 emissions and the green fraction for a wide spectrum of global cities (Nordbo et al, 2012; Velasco and Roth, 2010) revealed slightly differing patterns from that observed in our city. Consequently, the relationship based on eddy covariance data within a single city could be useful to evaluate CO_2 emissions at the city scale. The network of eddy covariance measurements within a city is a very powerful tool to evaluate CO_2 emissions in urban areas.

Acknowledgments

We thank Dr. Hiroyuki Kaga of Osaka Prefecture University for supporting the GIS analysis. We thank the people of Sakai City Office for supporting measurements at SAC. The measurements at IZM were supported by the Sumitomo Foundation (143205). The measurements at SAC were partly supported by Nissei Foundation grants for Environmental Problems, H21. Traffic data regarding Hanshin Expressway were provided by the Hanshin Expressway Company. Data on gas consumption by Osaka Prefecture University were provided by the university.

References

Awal, M.A., Ohta, T., Matsumoto, K., Toba, T., Daikoku, K., Hattori, S., Hiyama, T., Park, H., 2010. Comparing the carbon sequestration capacity of temperate deciduous forests between urban and rural landscapes in central Japan. Urb. For. Urb. Greening 9, 261-170.

Baldocchi, D., 2014. Measuring fluxes of trace gases and energy between ecosystems and the atmosphere –the state and future of the eddy covariance method. Glob. Change Biol. 20, 3600-3609.

Bergeron, O., Strachan, I.B., 2011. CO_2 sources and sinks in urban and suburban areas of a norther mid-latitude city. Atmos. Environ. 45, 1564-1573.

Canadell, J.G., Le Quéré, C., Raupach, M.R., Field, C.B., Buitenhuis, E.T., Ciais, P., Conway, T.J., Gillett, N.P., Houghton, R.A., Marland, G., 2007. Contributions to accelerating atmospheric CO_2 growth from economic activities, carbon intensity, and efficiency of natural sinks. Proc. Natl., Acad. Sci. 104, 18866-18870.

Coutts, A.M., Beringer, J., Tapper, N.J., 2007. Characteristics influencing the variability of urban CO_2 fluxes in Melbourne, Australia. Atmos. Environ. 41, 51-62.

Crawford, B., Grimmond, C.S.B., Christen, A., 2011. Five years of carbon dioxide fluxes measurements in a highly vegetated suburban area. Atmos. Environ. 45, 896-905.

Gioli, B., Toscano, P., Lugato, E., Matese, A., Miglietta, F., Zaldei, A., Vaccari, F.P., 2012. Methane and carbon dioxide fluxes and source partitioning in urban areas: the case study of Florence, Italy. Environ. Poull. 164, 125-131.

Gough, C.M., Vogel, C.S., Harrold, K.H., George, K., Curtis, P.S., 2007. The legacy of harvest and fire on ecosystem carbon storage in a north temperate forest. Global Change Biol. 13, 1935-1949.

Grimmond, C.S.B., King, T.S., Cropley, F.D., Nowak, D.J., Souch, C., 2002. Local-scale fluxes of carbon dioxide in urban environments: methodological challenges and results from Chicago. Environ. Pollut. 116, S243-S254.

Grimmond, C.S.B., Salmond, J.A., Oke, T.R., Offerle, B., Lemonsu, A., 2004. Flux and turbulence measurements at a densely built-up site in Marseille: heat, mass (water and carbon dioxide), and momentum. J. Geophys. Res. 109, doi:10.1029/2004JD004936.

Hirano, T., Kiyota, M., Aiga, I., 1996. Vegetation in Sakai City, Osaka, as a sink of air pollutants. Bull. Univ. Osaka Pref., Ser. B 48, 55-64.

Hirano, T., Sugawara, H., Murayama, S., Kondo, H., 2015. Diurnal variation of CO_2 flux in an urban area of Tokyo. SOLA 11, 100-103.

Järvi, L., Nordbo, A., Riikonen, A., Moilanen, J., Nikinmaa, E., Vesala, T., 2012. Seasonal and annual variation of carbon dioxide surface fluxes in Helsinki, Finland, in 2006-2010. Atmos. Chem. Phys., 12, 8475-8489.

Kochendorfer, J., Meyers, T.P., Frank, J., Massman, W.J., Heuer, M.W., 2012. How well can we measure the vertical wind speed? Implications for fluxes of energy and mass. Boundary-Layer Meteorol. 145, 383-398.

Kordowski, K., Kuttler, W., 2010. Carbon dioxide fluxes over an urban park area. Atmos. Environ. 44, 2722-2730.

Kormann, R., Meixner, F.X., 2000. An analytical footprint model for non-neutral stratification. Boundary-Layer Meteorol. 99, 207-224.

Kotthaus, S., Grimmond, C.S.B., 2012. Identification of micro-scale anthropogenic CO_2, heat and moisture sources – Processing eddy covariance fluxes for a dense urban environment. Atmos. Environ. 57, 301-316.

Latty, E.F., Canham, C.D., Marks, P.L., 2004. The effects of land-use history on soil properties and nutrient dynamics in northern hardwood forests of the Adriondack Mountains. Ecosystems 7, 193-207.

Liu, H.Z., Feng, J.W., Vesala, T., 2012. Four-year (2006-2009) eddy covariance measurements of CO_2 flux over an urban area in Beijing. Atmos. Chem. Phys., 12, 7881-7892.

Lloyd, J., Taylor, J.A., 1994. On the temperature dependence of soil respiration. Funct. Ecol. 8, 315-323.

Massman, W.J., 2000. A simple method for estimating frequency response corrections for eddy covariance systems. Agric. For. Meteorol. 104, 185-198.

Mills, G., 2007. Cities as agents of global change. Int., J. Climatol. 27, 1849-1857.

Moriwaki, R., Kanda, M., Nitta, H., 2006. Carbon dioxide build-up within a suburban canopy layer in winter night. Atmos. Environ. 40, 1394-1407.

Moore, C.J., 1986. Frequency response corrections for eddy correlation systems. Boundary-Layer Meteorol. 37, 17-35.

Nakai, T., Shimoyama, K., 2012. Ultrasonic anemometer angle of attack errors under turbulent conditions. Agric. For. Meteorol. 162-163, 14-26.

Nimitz, E., Hargreaves, K.J., McDonald, A.G., Dorsey, J.R., Fowler, D., 2002. Micrometeorological measurements of the urban heat budget and CO_2 emissions on a city scale. Environ. Sci. Technol. 36, 3139-3146.

Nordbo, A., Järvi, L., Haapanala, S., Wood, C. R., Vesala, T., 2012. Fraction of natural area as main predictor of net CO_2 emissions from cities. Goephys. Res. Lett. 39, doi:10.1029/2012GL053087.

Oda, T., Maksyutov, S., 2011. A very high-resolution (1 km × 1 km) global fossil fuel CO_2 emission inventory derived using a point source database and satellite observations of nighttime lights. Atmos. Chem. Phys. 11, 543-556.

Pawlak, W., Fortuniak, K., Siedlecki, M., 2011. Carbon dioxide flux in the center of Łódź, Poland –analysis of a 2-year eddy covariance measurement data set. Int. J. Climatol. 31, 232-243.

Peters, W., Jacobson, A.R., Sweeney, C., Andrews, A.E., Conway, T.J., Masarie, K., Miller, J., Bruhwiler, L.M., Pétron, G., Hirsch, A.I., Worthy, D.E.J., van der Werf, G.R., Randerson, J.T., Wennberg, P.O., Krol, M.C., Tans, P.P., 2007. An atmospheric perspective on North American carbon dioxide exchange: CarbonTracker. Proc. Natl., Acad. Sci. 104, 18925-18930.

Schimel, D.S., House, J.I., Hibbard, K.A., Bousquet, P., Ciais, P., Peylin, P., Braswell, B.H., Apps, M.J., Baker, D., Bondeau, A., Canadell, J., Churkina, G., Cramer, W., Denning, A.S., Field, C.B., Fridlingstein, P., Goodale, C., Heimann, M.,

Houghton, R.A., Melilo, J.M., Moore III, B., Murdiyarso, D., Noble, I., Pacala, S.W., Prentice, I.C., Raupach, M.R., Rayner, P.J., Scholes, R.J., Steffen, W.L., Wirth, C., 2001. Recent patterns and mechanisms of carbon exchange by terrestrial ecosystems. Nature 414, 169-172.

Stterthwite, D., 2008. Cities' contribution to global warming: notes on the allocation of global greenhouse gas emission. Environ. Urbanization, 20, 539-549.

Ueyama, M., Hirata, R., Mano, M., Hamotani, K., Harazono, Y., Hirano, T., Miyata, A., Takagi, K., Takahashi, Y., 2012. Influences of various calculation options on heat, water and carbon fluxes determined by open- and closed-path eddy covariance methods. Tellus 64B, 19048, doi.org/10.3402/tellusb.v64i0.19048.

Ueyama, M., Mitake, Y., Yamaguchi, K., Hamotani, K., 2011. Micrometeorological measurements of heat, water, and CO_2 exchanges at an urban landscape in Sakai, Japan. AsiaFlux Newsletter 32, 9-12.

Ueyama, M., Iwata, H., Harazono, Y., Euskirchen, E.S., Oechel, W.C., Zona, D., 2013. Growing season and spatial variations of carbon fluxes of Arctic and boreal ecosystems in Alaska. Ecol. Appl. 23, 1798-1816.

Velasco, E., Pressley, S., Allwine, E., Westberg, H., Lamb, B., 2005. Measurements of CO_2 fluxes from the Mexico City urban landscape. Atmos. Environ. 39, 7433-7446.

Velasco, E., Roth, M., 2010. Cities as net source of CO_2: review of atmospheric CO_2 exchange in urban environments measured by eddy covariance technique. Geography Compass 4/9, 1238-1259.

Ward, H.C., Evans, J.G., Grimmond, C.S.B., 2013. Multi-season eddy covariance observations of energy, water and carbon fluxes over a suburban area in Swindon, UK. Atmos. Chem. Phys. 13, 4645-4666.

Ward, H.C., Kotthaus, S., Grimmond, C.S.B., Bjorkegren, A., Wilkinson, M., Morrison, W.T.J., Evans, J.G., Morison, J.I.L., Iamarino, M. 2015. Effects of urban density on carbon dioxide exchanges: observations of dense urban, suburban and woodland areas of southern England. Environ. Pollut. 198, 189-200.

Webb, E.K., Pearman, G.I., Leuning, R., 1980. Correction of flux measurements for density effects due to heat and water vapour transfer. Quart. J. Roy. Meteorol. Soc. 106, 85-10.

Table 1: Annual CO₂ fluxes from the eddy covariance measurements and upscaled city-scale flux.

Site	CO_2 flux $g\ C\ m^{-2}\ yr^{-1}$
SAC west	4948
SAC east	3134
OPU	1270
IZM park	802
IZM rural	495
Upscale	3325
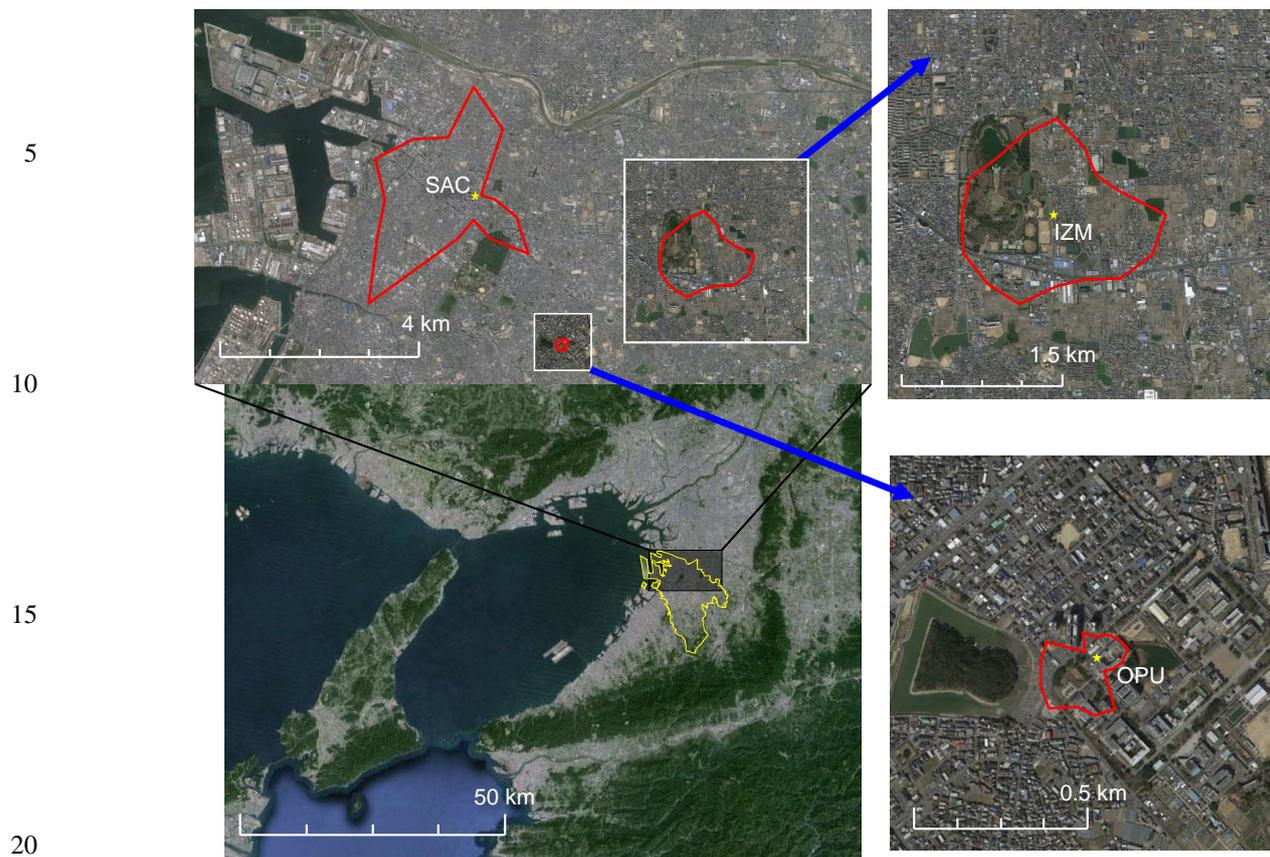
Figure 2: Aerial photograph by Google Earth showing the study area, where the 80% flux footprint in daytime is shown with red lines. The boundary of Sakai City is shown as a yellow line.

25
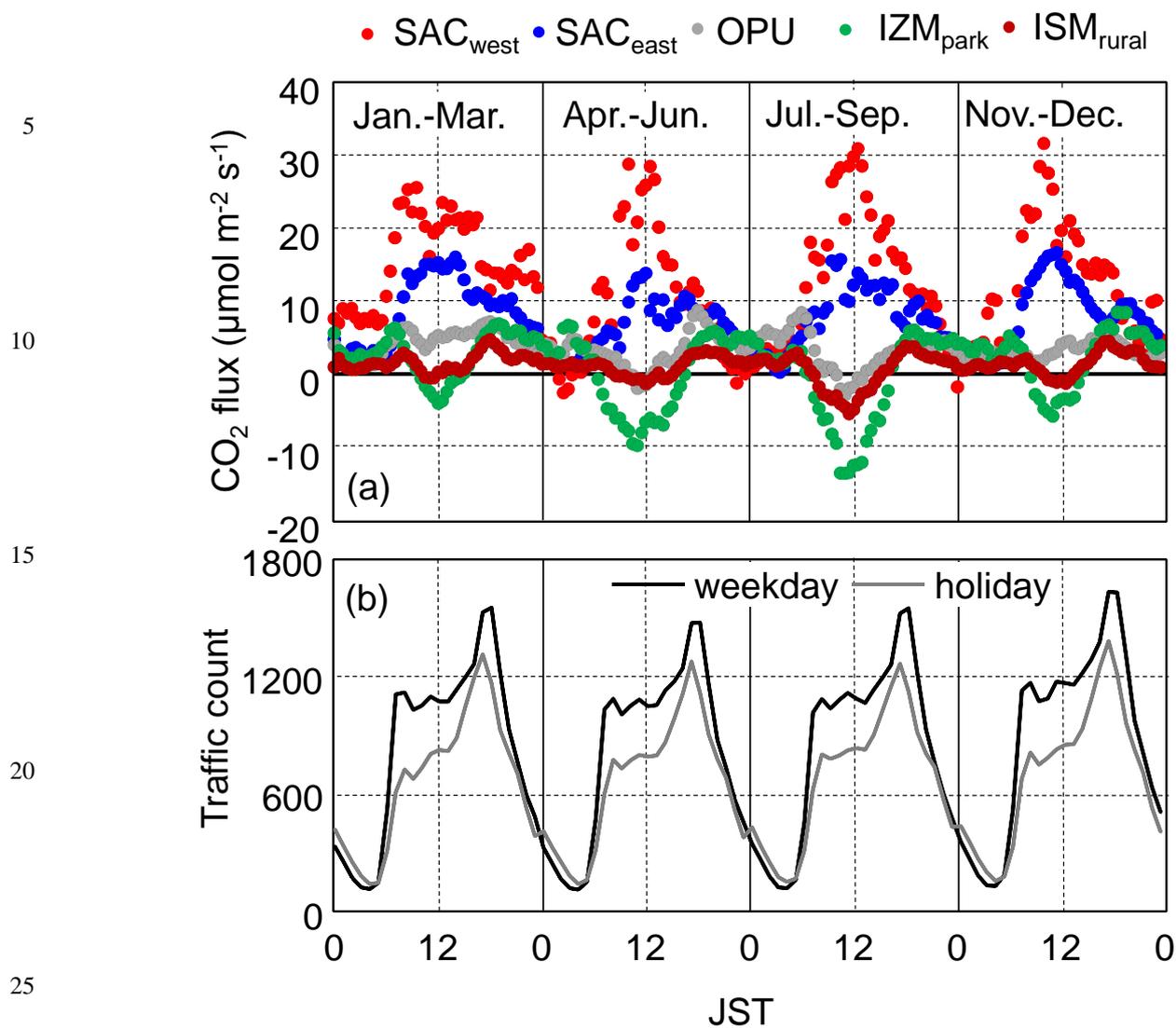
Figure 2: Mean diurnal variations of (a) CO₂ fluxes and (b) traffic count at two highway exits within the flux footprint of SAC west. The diurnal patters were created every consecutive three months in 2015. Because measurements at IZM began in February 2015, diurnal variations for IZM during the period from January to March were calculated based on data from February and March in 2015 and January in 2016.

25
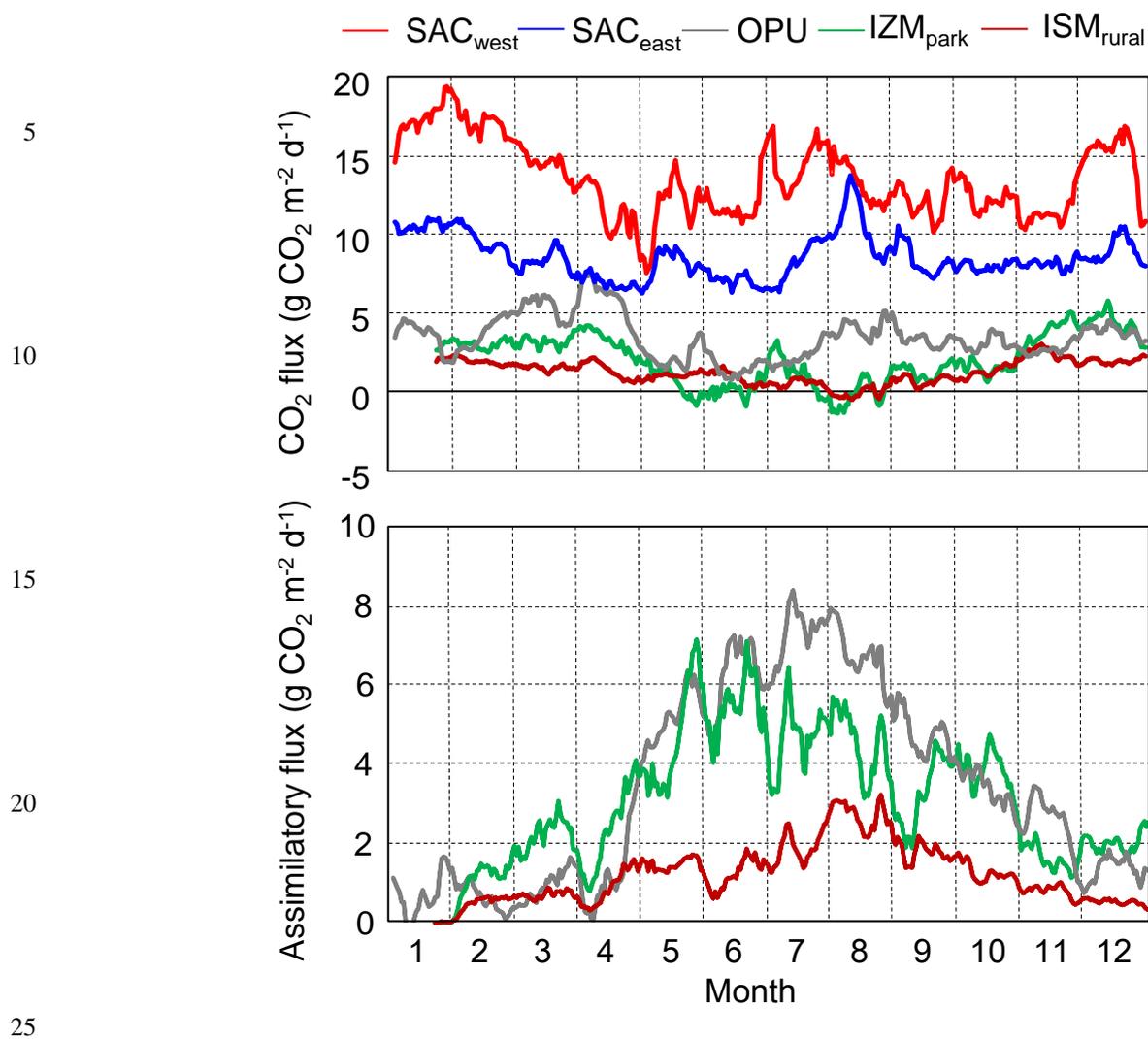
Figure 3: Seasonal variations of daily mean (a) CO_2 fluxes and (b) assimilatory flux in 2015, shown as a 7-day running mean.
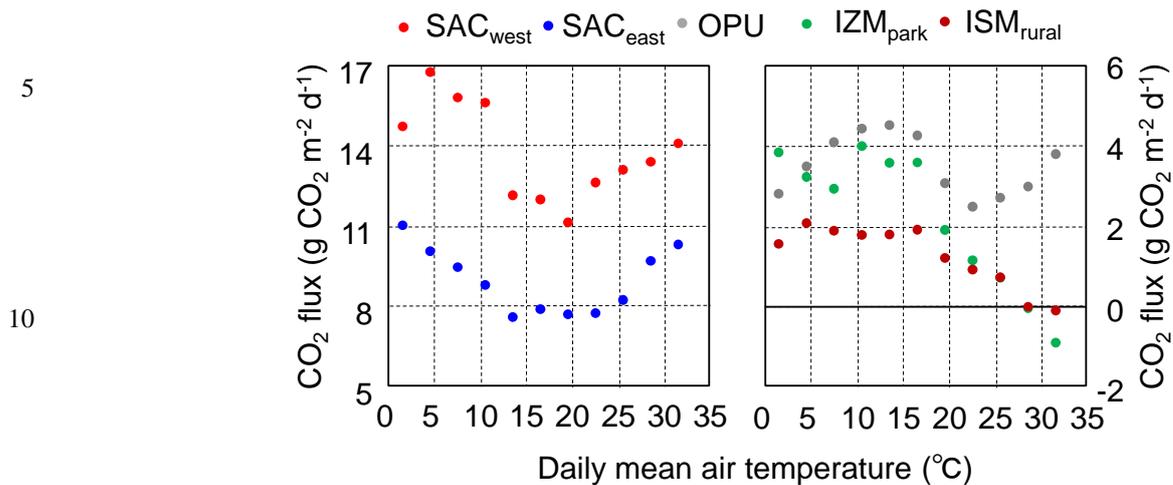
Figure 4: Relationship between daily mean air temperature and daily mean CO₂ flux; CO₂ flux data were binned with 3°C intervals.
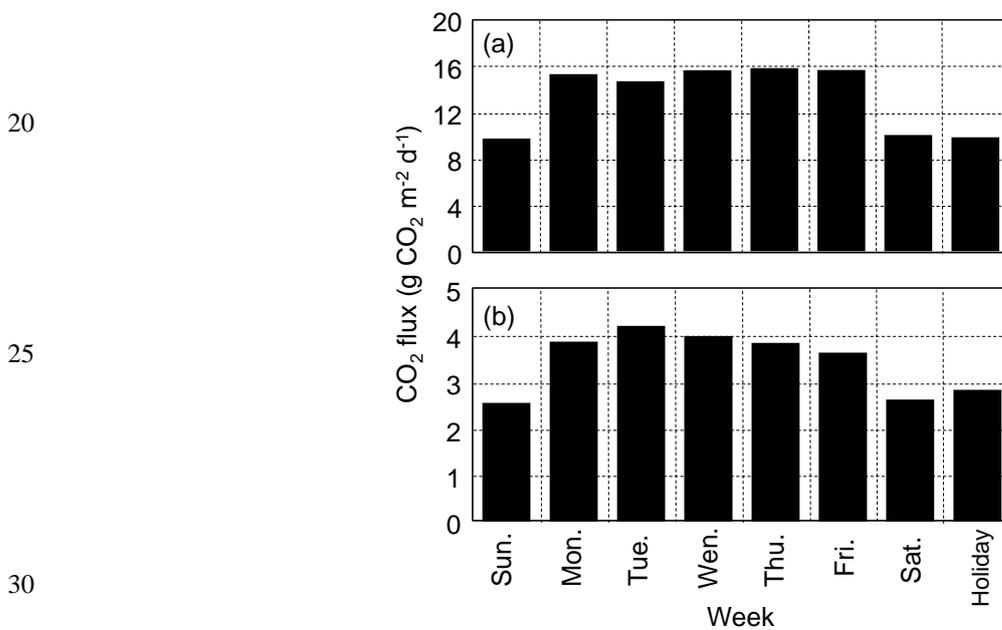
Figure 5: Averaged daily CO₂ flux for each day of the week in 2015 for (a) SAC west and (b) OPU; fluxes for holidays were separately averaged.
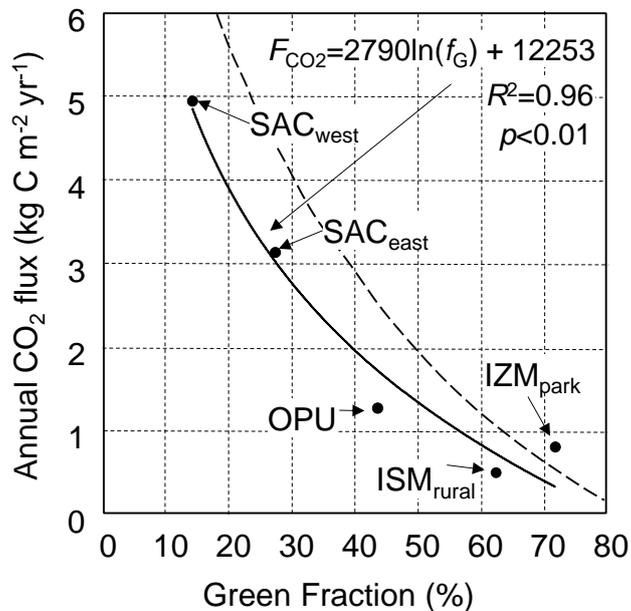
Figure 6: Relationship between annual CO_2 flux (F_{CO2}) and green fraction (f_G). The solid line represents regression based on our flux data for Sakai, and the dashed line represents a relationship based on a global synthesis (Nordbo et al., 2012).

25

30
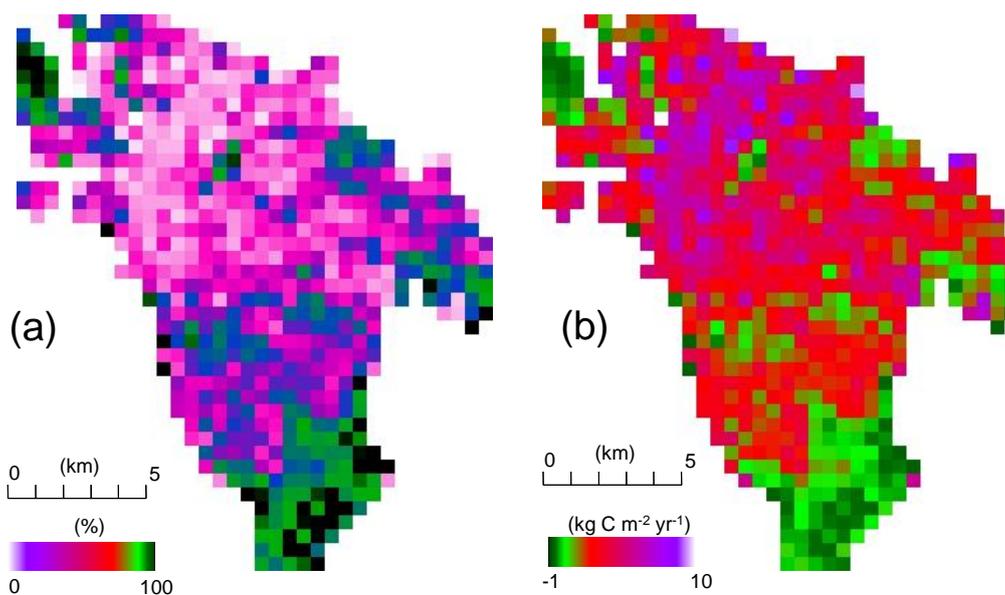
Figure 7: Spatial distributions of (a) green fraction and x (b) upscaled net CO_2 flu in Sakai City. The green fraction was calculated for a 500-m spatial resolution based on a inventory of green spaces.
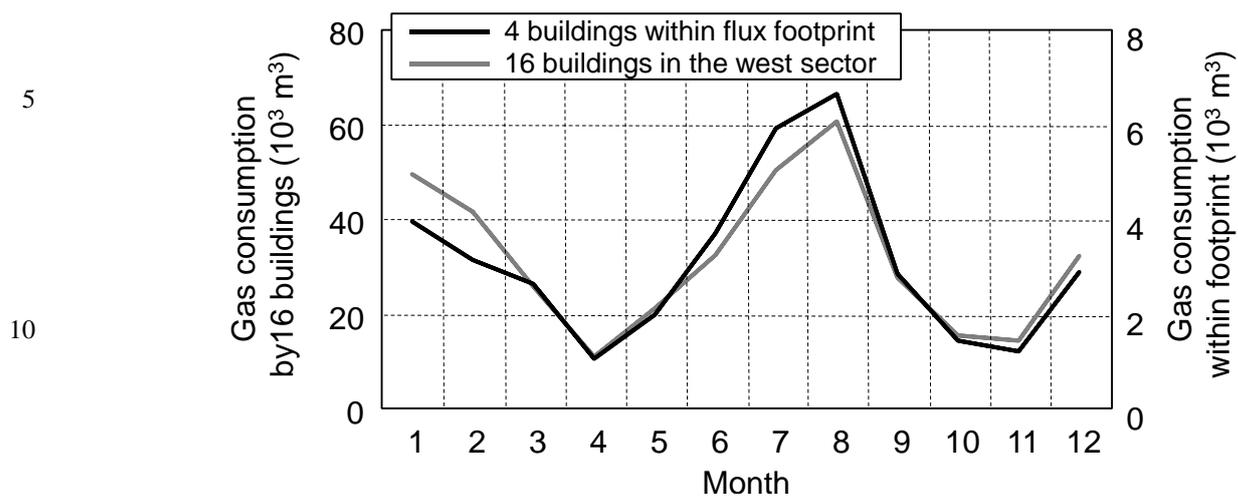
Figure A1: Seasonal variations in monthly gas consumption rates at Osaka Prefecture University for 2015. The data are shown for 16 buildings in the west-sector of the university, where flux measurements were conducted, and for four buildings located within the flux footprint.